Constraining *CP* Violating Nucleon-Nucleon Long-Range Interactions in Diatomic eEDM Searches

Chaja Baruch,[1,*] P. Bryan Changala,[2,†] Yuval Shagam,[3,‡] and Yotam Soreq[1,§]
[1]*Physics Department, Technion—Israel Institute of Technology, Haifa 3200003, Israel*
[2]*Center for Astrophysics | Harvard & Smithsonian, Cambridge, Massachusetts 02138, USA*
[3]*Schulich Faculty of Chemistry, The Helen Diller Quantum Center and the Solid State Institute, Technion—Israel Institute of Technology, Haifa 3200003, Israel*

(Received 23 February 2024; accepted 8 August 2024; published 13 September 2024)

The searches for *CP* violating effects in diatomic molecules, such as HfF^+ and ThO, are typically interpreted as a probe of the electron's electric dipole moment (*e*EDM), a new electron-nucleon interaction, and a new electron-electron interaction. However, in the case of a nonvanishing nuclear spin, a new *CP* violating nucleon-nucleon long-range force will also affect the measurement, providing a new interpretation of the *e*EDM experimental results. Here, we use the HfF^+ *e*EDM search and derive a new bound on this hypothetical interaction, which is the most stringent from terrestrial experiments in the 1 eV–10 keV mass range. These multiple new physics sources motivate independent searches in different molecular species for *CP* violation at low energy that result in model independent bounds, which are insensitive to cancellation among them.

DOI: 10.1103/PhysRevLett.133.113202

Introduction—Notwithstanding its great success, the standard model (SM) is not a complete description of nature and should be extended by physics beyond the standard model (BSM), which is well motivated both by observational evidence and strong theoretical arguments, see, e.g., [1]. New physics (NP) sources of *CP* violation (*CPV*) naturally appear in a variety of extensions of the SM and may be related to baryogenesis. Low energy BSM searches, e.g., [2], can probe these effects. In particular, *CPV* searches are sensitive to multiple NP effects, e.g., electric dipole moments (EDMs) [3–8]. Focusing on electron EDM (*e*EDM) searches in diatomic molecules, NP *CPV* can arise not only in the form of the *e*EDM, but also as a new *CPV* electron-nucleon (*eN*) or electron-electron (*ee*) interaction [9–12]. To date, the most stringent *e*EDM bound is $|d_e| < 4.1 \times 10^{-30}$ e cm [13,14], assuming no other *CPV* sources. This can be translated to new physics at the scale of $\mathcal{O}(10\ \text{TeV})$.

In this Letter, we point out that a new *CPV* nucleon-nucleon (*NN*) long-range force mediated by a spin-0 particle contributes to the *e*EDM frequency channel and that this effect is probed by measurements in diatomic molecules, in the case where one or both of the nuclei of the diatomic molecule have nonzero spin. This presents a set of models that are probed by reintepreting the current *e*EDM results. In addition to the *e*EDM, *CPV* can arise from long-range forces between electrons and nuclei, such that there are four NP *CPV* sources, namely, d_e, *eN*, *ee*, and *NN*. To constrain these four *CPV* sources, at least four independent measurements are required.

The three most sensitive *e*EDM searches in molecules are the JILA HfF^+ search [13], the ACME ThO search [15], and the Imperial College London YbF search [16,17]. Only the first and last include nuclei with nonvanishing spins and are sensitive to *NN*. We utilize these three searches to derive novel bounds on three NP *CPV* sources, i.e., d_e, *eN*, and *NN*. We note that *ee* contributes to d_e and directly through the measured frequency channel. The interaction can be also probed by atomic EDM searches [9] with decent precision. We neglect it here for simplicity and leave this comparison for future work. Our result is the most constraining bound on *NN* from terrestrial experiments, improving current constraints by up to 6 orders of magnitude in the 1 eV–10 keV mass range. Because the YbF *e*EDM bound is weaker by $\mathcal{O}(100)$ compared to the other *e*EDM searches sensitive to *NN*, the upcoming ThF^+ experiment [18], which also contains one nucleus with a nonzero spin, is further motivated and will lead to a 100-fold improved sensitivity. Astrophysical bounds from stellar cooling [19,20] and neutron stars [21] are stronger by 2–3 orders of magnitude, see also [22]. However, these

*Contact author: chajabaruch@campus.technion.ac.il
†Contact author: bryan.changala@cfa.harvard.edu
‡Contact author: yush@technion.ac.il
§Contact author: soreqy@physics.technion.ac.il

astrophysical bounds are subject to large systematic uncertainties and moreover, can be avoided in certain models, see below.

Long-range CPV force—We consider a new spin-0 particle, ϕ, with mass m_ϕ and both scalar and pseudoscalar couplings to fermions. The effective couplings between ϕ, the nucleons, $N = n,\ p$, and the electrons are given by

$$\mathcal{L}_{\mathrm{int}} \subset \sum_{\psi=e,p,n} \phi\left(g_{\mathrm{S}}^{\psi}\bar{\psi}\psi + i g_{\mathrm{P}}^{\psi}\bar{\psi}\gamma_5\psi\right), \qquad (1)$$

and can be mapped to UV models. For example, see [23] and [24,25] for a recent review on the CPV axion. If ϕ is the QCD axion the expected CPV is too small to be observed, see, e.g., [26,27]. Another example is relaxion models [28–30], which induce a CPV light scalar as a result of mixing with the SM-Higgs boson.

The effective couplings from Eq. (1) are constrained both by terrestrial experiments and astrophysical observations, see, e.g., [22,31]. For $m_\phi \lesssim 10$ keV, the most stringent bounds on the effective coupling come from stellar cooling $g_{\mathrm{S}}^{N} < 6.5 \times 10^{-13}$ [19], see also [20], from cooling of hot neutron stars $(g_{\mathrm{P}}^{n}, g_{\mathrm{P}}^{p}) < (1.3, 1.5) \times 10^{-9}$ [21] and from SN1987 $g_{\mathrm{P}}^{N} < 6.0 \times 10^{-10}$ [32]. It has been suggested that the SN1987 bound faces substantial uncertainties, casting doubt on its robustness [33]. All of these astrophysical bounds can be avoided in models that are subject to environmental effects, see, e.g., [34–39] and discussion in [22]. Additionally, the constraints we set in this work are weaker only by 2–3 orders of magnitude compared to the astrophysical constraints. Moreover, at the one-loop level, the scalar and pseudoscalar proton couplings contribute to the scalar-photon and pseudoscalar-photon couplings. Following Ref. [40] to translate the strongest bounds on these photon couplings, we obtain a bound of $\mathcal{O}(10^{-16})$ on $g_S^p g_P^p$. In this case, globular cluster bounds [41] are subject to the same ambiguity as mentioned above.

Considering terrestrial experiments, the most stringent bounds arise from the proton and neutron EDMs, $|d_p| < 2.1 \times 10^{-25}\ e\,\mathrm{cm}$ [42] and $|d_n| < 1.8 \times 10^{-26}\ e\,\mathrm{cm}$ [43,44], respectively. Following Ref. [25] and assuming $m_\phi \ll \mathrm{GeV}$, the bounds on the effective couplings of Eq. (1) are $g_{\mathrm{S}}^{p} g_{\mathrm{P}}^{p} < 8.4 \times 10^{-10}$ and $g_{\mathrm{S}}^{n} g_{\mathrm{P}}^{n} < 1.0 \times 10^{-10}$. Additional bounds via pion nucleon coupling lead to $g_{\mathrm{S}}^{n,p} g_{\mathrm{P}}^{n,p} < 10^{-9} - 10^{-11}$ [45]. For $m_\phi \lesssim \mathrm{eV}$ there are very stringent bounds from searches with macroscopic objects, e.g., [46–50], see discussion in [22]. The scalar and pseudoscalar couplings can be separately probed by CP conserving observables, such as molecular vibrational modes, e.g., [51,52] and rare kaon decays, e.g., [53]. The combined strongest laboratory bounds on the scalar coupling, from neutron scattering [54–57], and pseudoscalar coupling, from molecular HD [58], together give a constraint of $g_{\mathrm{S}}^{n} g_{\mathrm{P}}^{n} < 1.0 \times 10^{-16}$ for $m_\phi \lesssim 1$ eV and $g_{\mathrm{S}}^{n} g_{\mathrm{P}}^{n} < 1.0 \times 10^{-9} - 10^{-10}$ for the keV range. For additional bounds, see, e.g., [59]. Bounds on the CPV scalar-photon coupling can be found in, e.g., [60]. They can be reinterpreted as a bound on the proton coupling and the terrestrial bounds are found to be weaker than other relevant bounds in the keV range.

The effective monopole-dipole potential between two nuclei i and j is given by [61–63]

$$V_{\mathrm{SP}}(r) = \alpha_\phi^{ij} \frac{\vec{\sigma}_j \cdot \hat{r}}{2\bar{m}_N}\left(\frac{1}{r} + m_\phi\right)\frac{e^{-r m_\phi}}{r}, \qquad (2)$$

where $\vec{\sigma}_j$ are the Pauli matrices that follow the spin of the valance nucleon, $\bar{m}_N = 939$ MeV is the average nucleon mass, and $\vec{r}$ is the internuclear axis of the molecule. The NP interaction strength is defined

$$\alpha_\phi^{ij} \equiv -\frac{1}{4\pi}(Z^i g_{\mathrm{S}}^{p} + N^i g_{\mathrm{S}}^{n})(B_p^j g_{\mathrm{P}}^{p} + B_n^j g_{\mathrm{P}}^{n}), \qquad (3)$$

where $Z^i (N^i)$ is the number of protons (neutrons) in nucleus i. The relation between the nucleus and the nucleon spins, as well as the proton-neutron mass difference, is encoded in $B_{n,p}^{j}$ [62,64,65], see Supplemental Material [66]. Since for molecules $r \sim 10^{-10}$m, a ϕ with $m_\phi \lesssim 2$ keV will induce a long-range force at the molecular scale.

Nucleon-nucleon long-range CPV force in diatomic molecules—Here we briefly describe the recently reported eEDM measurement using trapped HfF^{+} molecules [13,14], which we use as an example to illustrate the effect. The measurement is focused on the $^3\Delta_1$, $J = 1$, $F = 3/2$ science state. Leveraging the $^3\Delta_1$ state's Ω doubling, the state is polarized by a rotating electric field to form states of well-defined orientation, called the upper and lower doublets, denoted by $\Omega m_F = \pm 3/2$, see Fig. 1(a). Here $\Omega = \pm 1$ denotes the quantum number of the projection of the electronic angular momentum, $J = L + S = 1$, onto the internuclear axis in the molecule frame and m_F is the quantum number of the projection of the total angular momentum including nuclear spin, $F = J + I$, in the rotating frame. A bias magnetic field is aligned or anti-aligned with the electric field to lift the remaining degeneracy between the $m_F = \pm 3/2$ states of both $\Omega m_F = \pm 3/2$ doublets, Fig. 1(b). In total there are four relevant states, $|\Omega, m_F\rangle = |\pm 1, \pm 3/2\rangle$.

The energy of each state is a sum of a common energy shift (E_0), a state dependent Stark shift (E_{S}), Zeeman shift (E_{Z}) and a CPV shift (E_{CPV}), which includes the eEDM and other NP effects. In total, we can write

$$E_{\Omega,m_F} = E_0 + E_{\mathrm{S}} + E_{\mathrm{Z}} + E_{CPV}. \qquad (4)$$

The signs of E_{S}, E_{Z}, and E_{CPV} are proportional to the signs of Ωm_F, $m_F B_0$, and Ωm_F^2, respectively, where B_0 is the magnetic field. The sign of the Stark shift follows the orientation of the molecule axis relative to the rotating

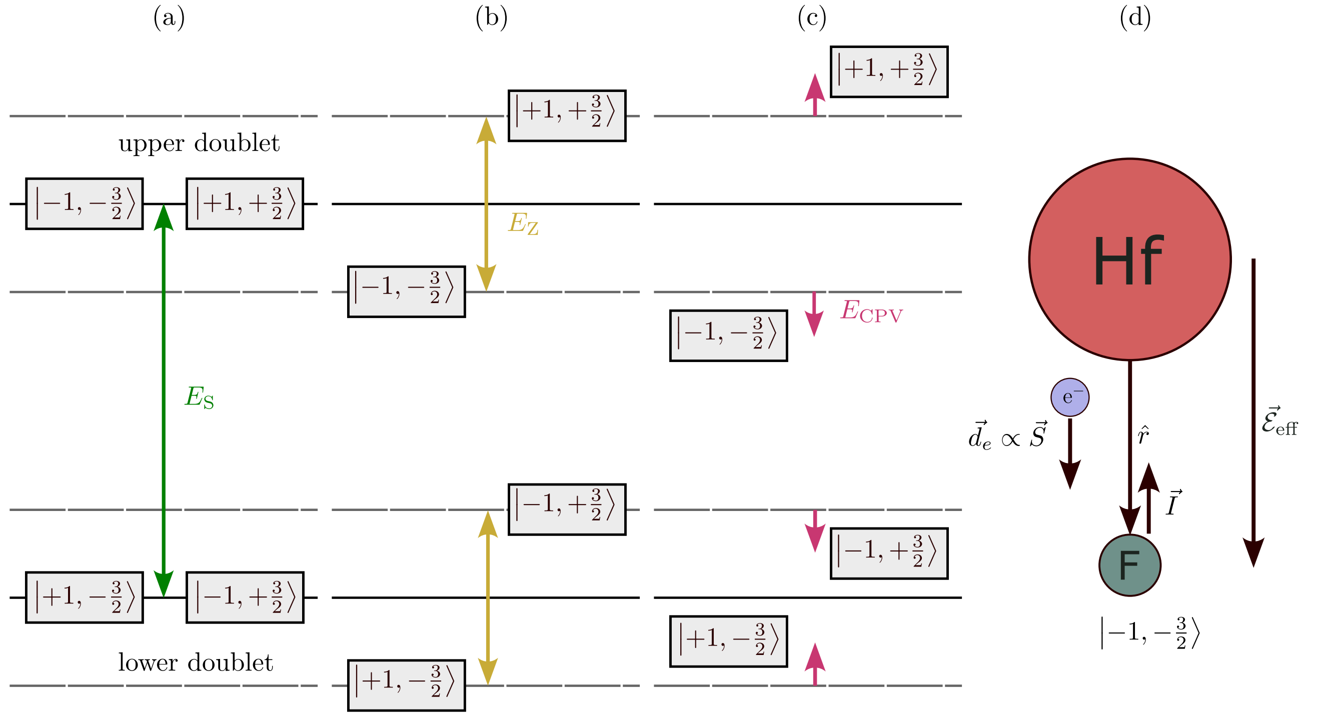

FIG. 1. The splitting of the energy levels, $|\Omega, m_F\rangle$, is shown when applying an electric field in (a), a parallel electric and magnetic field in (b) and the additional shift due to E_{CPV}, i.e., eEDM, NN, and eN, is shown in (c). The relative directions are illustrated in (d). See main text for details.

frame, which is defined by the rotating electric field. The Zeeman shift follows the orientation of the electron spin relative to the rotating frame, which is aligned with the magnetic field. The CPV is proportional to both $\Omega m_F \times m_F$, i.e., to the product of the external electric and magnetic fields.

In an example iteration of the experiment, the molecules are prepared in the $|\pm 1, +3/2\rangle$ states. A Ramsey spin-precession measurement is conducted between the $m_F = +3/2$ and $-3/2$ states for the two doublets with the results measured separately. Here E_0 and E_S are common to the $m_F = \pm 3/2$ states and are canceled to leading order where residual effects are suppressed. For a positive E_{CPV}, the two states $m_F = \pm 3/2$ with opposite Ω move closer together (farther apart) in lower, $\Omega m_F = -\frac{3}{2}$ (upper, $\Omega m_F = \frac{3}{2}$) doublets, Fig. 1(c). The doubly differential measurement between the results for the two doublets as well as the aligned and antialigned magnetic fields is used to isolate the CPV effects. Thus, under $(B_0, m_F, \Omega m_F) \to (-B_0, -m_F, -\Omega m_F)$ (or in other words, the f_{DB} channel) we are left with

$$E_{CPV} = \frac{(E_{+1,+\frac{3}{2}} - E_{-1,-\frac{3}{2}}) - (E_{-1,+\frac{3}{2}} - E_{+1,-\frac{3}{2}})}{4}, \quad (5)$$

and the sign of B_0 is same as the sign of m_F. The measurements from other experimental switches are averaged to suppress sources of systematic uncertainty, which are not written in Eq. (4) for simplicity.

The principle of the measurement illustrated above is common to all eEDM experiments such as HfF^+, ThO, and ThF^+ where Ω doubling is in effect. In other cases such as YbF, the electric field direction is switched instead of comparing doublet states. In all these cases, fully stretched states of the total angular momentum F are used to orient the eEDM with respect to the molecule, whose strong internal electric fields polarize to the electron. This effective electric field, $\vec{\mathcal{E}}_{\rm eff}$, points along the $\hat{r}$ direction, i.e., $\hat{r} \sim \Omega m_F$. This means that any nonzero nuclear spin, namely, that of ^{19}F ($I = 1/2$), will be oriented with both the eEDM and the internuclear axis.

Next, we describe why this measurement is also sensitive to the CPV NN interaction. In the eEDM experiment, the polarizing electric field $E_{\rm rot}$ is parallel or antiparallel to the magnetic field $B_{\rm rot}$. Moreover, for $F = 3/2$, the nuclear spin of fluorine must be oriented with J. Thus, for the fully stretched m_F states the nuclear spin points along the internuclear axis and against the electron spin.

More explicitly, the energy shift of the eEDM $\propto \langle \vec{\mathcal{E}}_{\rm eff} \cdot \vec{d}_e \rangle \propto \langle \hat{r} \cdot \vec{S} \rangle \propto \langle \hat{r} \cdot \vec{I} \rangle \propto V_{\rm PS}$ of Eq. (2) for each of the 4 states with I the nuclei spin. Therefore, the effect of Eq. (2) behaves as $V_{\rm PS} \propto \langle \hat{r} \cdot \vec{I} \rangle \propto \Omega m_F \times m_F \propto \Omega m_F^2$. This means that for the upper (lower) doublet the states

TABLE I. Summary of eEDM measurements and the parameters relevant to computing the NN coupling effect. W_{eN}^{ij} and W_{NN}^{ij} are given in the limit of $m_\phi \ll$ keV.

Molecule	r_{eq} [Å]	W_{NN}^{ij} [μHz]	$W_{d_e}^{ij}$ [μHz/e cm]	W_{eN}^{ij} [μHz]	E_{CPV}^{ij} [μHz]
$^{180}HfF^+$	1.81 [68]	1.55×10^{17}	5.55×10^{30} [10]	1.16×10^{22} [9]	-7.3 ± 11.9 [13]
^{232}ThO	1.84 [69]	···	1.91×10^{31} [10]	1.03×10^{22} [9]	81.2 ± 77.2 [15]
^{174}YbF	2.02 [69]	1.24×10^{17}	-3.12×10^{30} [10]	2.21×10^{22} [9]	748.7 ± 1810.5 [16]
$^{232}ThF^+$	1.99 [70]	1.28×10^{17}	9.02×10^{30} [71]		0 ± 5 (projection) [18]

$m_F = \pm 3/2$ move closer together (farther apart) in energy due the V_{PS} interaction for $g_{\mathrm{P}}^N g_{\mathrm{S}}^N > 0$, which is exactly the ($\mathcal{T}$-violating) behavior of the eEDM and their contributions to the E_{CPV} energy cannot be distinguished. The splitting of the energy levels when applying electromagnetic fields is shown in Figs. 1(a)–1(b). Therefore, in addition to d_e, and CPV in eN and ee interactions [9–11], the diatomic eEDM searches can be affected also from NN CPV long-range forces as captured by the potential of Eq. (2).

The four relevant CPV sources in the diatomic molecule ij can be written as

$$E_{CPV}^{ij} = W_{d_e}^{ij} d_e + W_{eN}^{ij} \alpha_\phi^{ie} + W_{ee}^{ij} \alpha_\phi^{ee} + W_{NN}^{ij} \alpha_\phi^{ij}, \quad (6)$$

where the eN, ee, and NN contributions are functions of m_ϕ, $\alpha_\phi^{ie} \equiv (Z^i g_{\mathrm{S}}^p + N^i g_{\mathrm{S}}^n) g_{\mathrm{P}}^e / 4\pi$, and $\alpha_\phi^{ee} \equiv g_{\mathrm{S}}^e g_{\mathrm{P}}^e / 4\pi$. The $W_{NN}^{ij} \alpha_\phi^{ij}$ is the new CPV nucleon-nucleon interaction due to the potential in Eq. (2). The relevant W^{ij}'s are summarized in Table I with other experimental values, see also [11] for $W_{eN}^{\mathrm{HfF}^+}$ and $W_{ee}^{\mathrm{HfF}^+}$. Since the ee interaction can be directly probed by atomic systems, e.g., [9], and contributes also to the eEDM, we neglect it below, but it is straightforward to include. We note that the eN interaction can also be probed by atomic systems, see, e.g., [9,67].

The nucleon-nucleon interaction function can be estimated by using first-order perturbation theory

$$W_{NN}^{ij} = \frac{\langle V_{\mathrm{SP}} \rangle}{\alpha_\phi^{ij}} \approx \frac{\langle \vec{\sigma}_j \cdot \hat{r}_{\mathrm{eq}} \rangle}{2\bar{m}_N} \left(\frac{1}{r_{\mathrm{eq}}} + m_\phi \right) \frac{e^{-r_{\mathrm{eq}} m_\phi}}{r_{\mathrm{eq}}}, \quad (7)$$

where r_{eq} is the equilibrium distance between the two nuclei and $\langle \vec{\sigma}_j \cdot \hat{r}_{\mathrm{eq}} \rangle$ is the nuclear spin expectation value on the internuclear axis for the state. In the fully stretched state (maximal angular momentum), $\langle \vec{\sigma}_j \cdot \hat{r}_{\mathrm{eq}} \rangle = 1$. Although we have taken the internuclear distance to be fixed to its equilibrium value, we have verified, using the Morse anharmonic potential, that the correction from consideration of the nuclear vibrational wave functions of the ground state is at the few percent level for most of the relevant m_ϕ range and at most $\mathcal{O}(1)$ for the high masses.

To further emphasize the importance of the NN effect and encourage future CPV measurements in new molecules, we estimate the possible limit that will likely be set in the mature ThF^+ measurement, assuming that a value consistent with zero is found. To predict the limit for ThF^+, we use the description in [18] to achieve a conservative estimate of the expected precision assuming a shot noise limited measurement. Reference [18] predicts a coherence time of 20 s and Ref. [72] reports 10 ions counted per shot on the side of the fringe in both doublets in

TABLE II. Summary of results, with 90% C.L. The columns indicate which interactions are switched on, see Eq. (6). The rows indicate the relevant couplings, for: only proton coupling (a), only neutron coupling (b), or equal proton and neutron couplings (c). For the eEDM the results for (a), (b), (c) differ by less than 10 percent.

	Measured (HfF$^+$, ThO, YbF)			Projection (HfF$^+$, ThO, YbF, ThF$^+$)	
	NN	NN, d_e	NN, d_e, eN	NN	NN, d_e
(a) $g_S^p g_P^p$	2.8×10^{-17}	7.6×10^{-17}	3.8×10^{-15}	8.8×10^{-18}	7.1×10^{-17}
(b) $g_S^n g_P^n$	2.5×10^{-16}	6.8×10^{-16}	3.1×10^{-14}	7.6×10^{-17}	6.6×10^{-16}
(c) $g_S^{p,n} g_P^{p,n}$	1.2×10^{-17}	3.3×10^{-17}	1.6×10^{-15}	3.7×10^{-18}	3.1×10^{-17}
d_e		1.1×10^{-29}	3.6×10^{-28}		8.5×10^{-30}
(a) $g_S^p g_P^e$			8.3×10^{-20}		
(b) $g_S^n g_P^e$			5.4×10^{-20}		
(c) $g_S^{p,n} g_P^e$			3.3×10^{-20}		

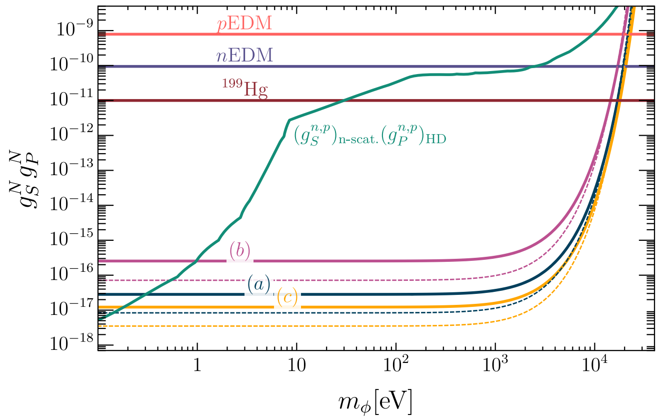

FIG. 2. The bounds on long-range nucleon-nucleon *CPV* interaction for only proton interaction (a), only neutron interaction (b), and both proton and neutron interaction (c). Bounds from neutron and proton EDMs [25], from ^{199}Hg [45], as well as the combined strongest laboratory bounds on the scalar coupling, from neutron scattering [54–57], and pseudoscalar coupling, from molecular HD [58], are also shown. Projected bounds due to a future ThF^+ measurement are plotted in dashed lines.

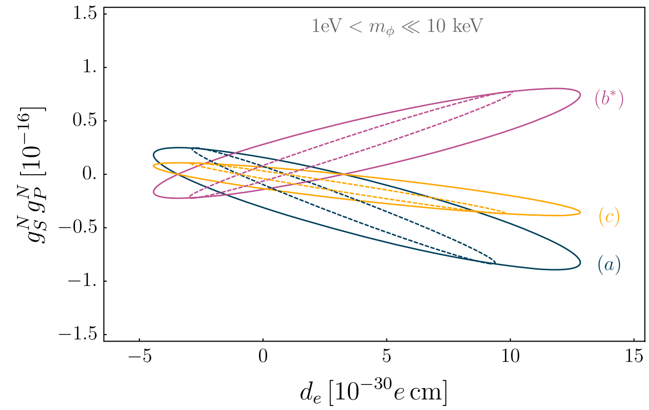

FIG. 3. The allowed region in the d_e–*NN* plane, when setting the electron-nucleon interaction to zero ($\alpha_\phi^{ie} = 0$), for 1 eV $< m_\phi \ll 10$ keV. The solid lines are derived from measurements of HfF^+ and ThO, and the dotted lines are derived from the measurement of HfF^+ and the projection of ThF^+. All three cases are plotted here, as indicated in the plot. Note that for (b), we rescaled the contour by a factor of 10 along the $g_S^N g_P^N$ axis.

a comparable measurement system. We also assume the fringe contrast is 0.55 as was found for HfF^+ [13] due to the similarities between the two systems. If a total of 600 h of data as in Ref. [13] are taken using the conveyor belt of ion traps architecture mentioned in Refs. [18,72], which would allow for a 10 Hz repetition rate, a total of 10^8 ions will be detected neglecting dead times and early time phase measurements. Using these parameters we predict a statistical uncertainty of $\sim 5\ \mu$Hz which we use for the projection here, see Table I.

Results—To set bounds on the couplings under consideration in this work, we use the measured frequency shift of HfF^+, ThO, and YbF. Additionally, we give projected bounds when considering the future ThF^+ measurement. This improves the sensitivity for the scenario in which all interactions are turned on by nearly 2 orders of magnitude.

We first consider the case of only the *NN* interaction and set the other *CPV* sources to zero. As there is only one unknown, namely, $g_S^N g_P^N$, it is sufficient to use only one *e*EDM measurement, the JILA HfF^+. We take into account three representative cases that illustrate the importance of the different coupling constants; ϕ interacts (a) only with protons, $g_S^n = g_P^n = 0$; (b) only with neutrons, $g_S^p = g_P^p = 0$; and (c) equally with protons and neutrons, $g_S^p = g_S^n$ and $g_P^p = g_P^n$. The resulting 90% confidence limit (C.L) upper bounds for $m_\phi \ll$ keV are given in Table II, and bounds as a function of m_ϕ are plotted in Fig. 2. This results in the strongest terrestrial bounds, to the best of our knowledge. For example, the bounds from the proton and neutron EDMs are weaker by at least 6 orders of magnitude. However, astrophysical bounds from stellar cooling are stronger by 3 or 4 orders of magnitude but are subject to different systematics and are model dependent, see the above discussion.

Second, we consider d_e and *NN* as *CPV* sources and assume vanishing ϕ–e couplings. In this scenario, we probe d_e and $g_S^N g_P^N$. Profiling with respect to each parameter and taking the $m_\phi \ll 10$ keV limit, the 90% C.L. intervals are given in Table II. The allowed region in the $g_S^N g_P^N$–d_e plane is shown in Fig. 3, with solid lines for the measurement result and dashed lines for the projection. The translated bounds for the aforementioned cases, (a),(b),(c), are given in Table II.

Third, we consider three *CPV* sources, d_e, *NN*, and *eN*. For simplicity, we take the limit of $m_\phi \ll$ keV, generalization for higher mass is straightforward. Profiling each time on the other parameter, the 90% C.L. intervals are given in Table II. The allowed regions in the $g_S^{n,p} g_P^e$–d_e, $g_S^{n,p} g_P^{n,p}$–d_e and $g_S^{n,p} g_P^e$–$g_S^{n,p} g_P^{n,p}$ planes can be found in the Supplemental Material [66].

Conclusions—In this work, we point out that the *e*EDM searches in diatomic molecules, composed of at least one nucleus with a nonvanishing spin, are sensitive to new long-range *CPV* nucleon-nucleon interactions, thus, proposing a new set of NP models that can be probed with *e*EDM searches. Based on the *e*EDM searches in HfF^+, ThO, and YbF, we have derived novel bounds on such a hypothetical interaction mediated by a spin-0 particle with scalar and pseudo-scalar couplings to nucleons. The resulting bounds are the most stringent obtained from laboratory experiments, improving existing limits by 6 orders of magnitude in the 1 eV–10 keV mass range. For example, we show that in the presence of *eN* and *NN* the bound on the d_e will be weaker by 2 orders of magnitude compared to the simple case of only *e*EDM as a source of *CPV*. We project that adding the expected ThF^+ measurement will improve the sensitivity by about 2 orders of magnitude.

There are two questions left for future work which we note. For *e*EDM searches using polyatomic molecules that rely on *l* doubling, the sensitivity to the *NN* effect needs to be determined from the direction of the nuclear spin, e.g., [73,74]. *e*EDM searches on excited rotational and vibrational states can vary the magnitude of the *NN* interaction contribution providing more information within a single molecule to isolate the effect.

Acknowledgments—We gratefully thank Yevgeny Stadnik for careful reading of the manuscript and fruitful discussions. We also thank Gilad Perez and Tomer Volansky for useful discussions. We thank Eric Cornell, Gilad Perez, Jun Ye for comments on the manuscript. C. B. and Y. So. are supported by Grants from the NSF-BSF (Grant No. 2021800), the ISF (Grant No. 483/20), the BSF (Grant No. 2020300) and by the Azrieli foundation. Y. Sh. gratefully acknowledges funding by the European Union (ERC, 101116032—Q-ChiMP). Views and opinions expressed are however those of the authors only and do not necessarily reflect those of the European Union or the European Research Council Executive Agency. Neither the European Union nor the granting authority can be held responsible for them.

[1] R. K. Ellis *et al.*, Physics briefing book: Input for the European strategy for particle physics update 2020, arXiv:1910.11775.

[2] M. S. Safronova, D. Budker, D. DeMille, D. F. Jackson Kimball, A. Derevianko, and C. W. Clark, Search for new physics with atoms and molecules, Rev. Mod. Phys. **90**, 025008 (2018).

[3] M. Pospelov, *CP* odd interaction of axion with matter, Phys. Rev. D **58**, 097703 (1998).

[4] J. S. M. Ginges and V. V. Flambaum, Violations of fundamental symmetries in atoms and tests of unification theories of elementary particles, Phys. Rep. **397**, 63 (2004).

[5] M. Pospelov and A. Ritz, Electric dipole moments as probes of new physics, Ann. Phys. (Amsterdam) **318**, 119 (2005).

[6] J. Engel, M. J. Ramsey-Musolf, and U. van Kolck, Electric dipole moments of nucleons, nuclei, and atoms: The standard model and beyond, Prog. Part. Nucl. Phys. **71**, 21 (2013).

[7] T. E. Chupp, P. Fierlinger, M. J. Ramsey-Musolf, and J. T. Singh, Electric dipole moments of atoms, molecules, nuclei, and particles, Rev. Mod. Phys. **91**, 015001 (2019).

[8] K. Gaul and R. Berger, Global analysis of *CP*-violation in atoms, molecules and role of medium-heavy systems, arXiv:2312.08858.

[9] Y. V. Stadnik, V. A. Dzuba, and V. V. Flambaum, Improved limits on axionlike-particle-mediated *P*, *T*-violating interactions between electrons and nucleons from electric dipole moments of atoms and molecules, Phys. Rev. Lett. **120**, 013202 (2018).

[10] T. Fleig and M. Jung, Model-independent determinations of the electron EDM and the role of diamagnetic atoms, J. High Energy Phys. 07 (2018) 012.

[11] S. D. Prosnyak, D. E. Maison, and L. V. Skripnikov, Updated constraints on, -violating axionlike-particle-mediated electron–electron and electron–nucleus interactions from HfF^+ experiment, Symmetry **15**, 1043 (2023).

[12] V. V. Flambaum, M. Pospelov, A. Ritz, and Y. V. Stadnik, Sensitivity of EDM experiments in paramagnetic atoms and molecules to hadronic *CP* violation, Phys. Rev. D **102**, 035001 (2020).

[13] T. S. Roussy *et al.*, An improved bound on the electron's electric dipole moment, Science **381**, adg4084 (2023).

[14] L. Caldwell *et al.*, Systematic and statistical uncertainty evaluation of the HfF^+ electron electric dipole moment experiment, Phys. Rev. A **108**, 012804 (2023).

[15] ACME Collaboration, Improved limit on the electric dipole moment of the electron, Nature (London) **562**, 355 (2018).

[16] J. J. Hudson, D. M. Kara, I. J. Smallman, B. E. Sauer, M. R. Tarbutt, and E. A. Hinds, Improved measurement of the shape of the electron, Nature (London) **473**, 493 (2011).

[17] D. M. Kara, I. J. Smallman, J. J. Hudson, B. E. Sauer, M. R. Tarbutt, and E. A. Hinds, Measurement of the electron's electric dipole moment using YbF molecules: Methods and data analysis, New J. Phys. **14**, 103051 (2012).

[18] K. B. Ng *et al.*, Spectroscopy on the electron-electric-dipole-moment–sensitive states of ThF^+, Phys. Rev. A **105**, 022823 (2022).

[19] S. Bottaro, A. Caputo, G. Raffelt, and E. Vitagliano, Stellar limits on scalars from electron-nucleus bremsstrahlung, J. Cosmol. Astropart. Phys. 07 (2023) 071.

[20] E. Hardy and R. Lasenby, Stellar cooling bounds on new light particles: Plasma mixing effects, J. High Energy Phys. 02 (2017) 033.

[21] M. Buschmann, C. Dessert, J. W. Foster, A. J. Long, and B. R. Safdi, Upper limit on the QCD axion mass from isolated neutron star cooling, Phys. Rev. Lett. **128**, 091102 (2022).

[22] C. A. J. O'Hare and E. Vitagliano, Cornering the axion with *CP*-violating interactions, Phys. Rev. D **102**, 115026 (2020).

[23] J. E. Moody and F. Wilczek, New macroscopic forces?, Phys. Rev. D **30**, 130 (1984).

[24] L. Di Luzio, H. Gisbert, G. Levati, P. Paradisi, and P. Sørensen, *CP*-violating axions: A theory review, arXiv:2312.17310.

[25] L. Di Luzio, G. Levati, and P. Paradisi, The chiral Lagrangian of *CP*-violating axion-like particles, J. High Energy Phys. 02 (2024) 020.

[26] S. Okawa, M. Pospelov, and A. Ritz, Long-range axion forces and hadronic *CP* violation, Phys. Rev. D **105**, 075003 (2022).

[27] W. Dekens, J. de Vries, and S. Shain, *CP*-violating axion interactions in effective field theory, J. High Energy Phys. 07 (2022) 014.

[28] P. W. Graham, D. E. Kaplan, and S. Rajendran, Cosmological relaxation of the electroweak scale, Phys. Rev. Lett. **115**, 221801 (2015).

[29] R. S. Gupta, Z. Komargodski, G. Perez, and L. Ubaldi, Is the relaxion an axion?, J. High Energy Phys. 02 (2016) 166.

[30] T. Flacke, C. Frugiuele, E. Fuchs, R. S. Gupta, and G. Perez, Phenomenology of relaxion-Higgs mixing, J. High Energy Phys. 06 (2017) 050.

[31] C. O'Hare, cajohare/AxionLimits: AxionLimits, https://cajohare.github.io/AxionLimits/ (2020).

[32] P. Carenza, T. Fischer, M. Giannotti, G. Guo, G. Martínez-Pinedo, and A. Mirizzi, Improved axion emissivity from a supernova via nucleon-nucleon bremsstrahlung, J. Cosmol. Astropart. Phys. 10 (2019) 016; 05 (2020) E01.

[33] N. Bar, K. Blum, and G. D'Amico, Is there a supernova bound on axions?, Phys. Rev. D **101**, 123025 (2020).

[34] C. Burrage and J. Sakstein, A compendium of chameleon constraints, J. Cosmol. Astropart. Phys. 11 (2016) 045.

[35] E. Masso and J. Redondo, Evading astrophysical constraints on axion-like particles, J. Cosmol. Astropart. Phys. 09 (2005) 015.

[36] J. Jaeckel, E. Masso, J. Redondo, A. Ringwald, and F. Takahashi, The need for purely laboratory-based axion-like particle searches, Phys. Rev. D **75**, 013004 (2007).

[37] W. DeRocco, P. W. Graham, and S. Rajendran, Exploring the robustness of stellar cooling constraints on light particles, Phys. Rev. D **102**, 075015 (2020).

[38] R. Budnik, H. Kim, O. Matsedonskyi, G. Perez, and Y. Soreq, Probing the relaxed relaxion and Higgs portal scenarios with XENON1T scintillation and ionization data, Phys. Rev. D **104**, 015012 (2021).

[39] I. M. Bloch, A. Caputo, R. Essig, D. Redigolo, M. Sholapurkar, and T. Volansky, Exploring new physics with O(keV) electron recoils in direct detection experiments, J. High Energy Phys. 01 (2021) 178.

[40] P. Escribano and A. Vicente, Ultralight scalars in leptonic observables, J. High Energy Phys. 03 (2021) 240.

[41] M. J. Dolan, F. J. Hiskens, and R. R. Volkas, Advancing globular cluster constraints on the axion-photon coupling, J. Cosmol. Astropart. Phys. 10 (2022) 096.

[42] B. K. Sahoo, Improved limits on the hadronic and semi-hadronic *CP* violating parameters and role of a dark force carrier in the electric dipole moment of ^{199}Hg, Phys. Rev. D **95**, 013002 (2017).

[43] C. Abel *et al.*, Measurement of the permanent electric dipole moment of the neutron, Phys. Rev. Lett. **124**, 081803 (2020).

[44] J. M. Pendlebury *et al.*, Revised experimental upper limit on the electric dipole moment of the neutron, Phys. Rev. D **92**, 092003 (2015).

[45] S. Mantry, M. Pitschmann, and M. J. Ramsey-Musolf, Distinguishing axions from generic light scalars using electric dipole moment and fifth-force experiments, Phys. Rev. D **90**, 054016 (2014).

[46] J. Lee, A. Almasi, and M. Romalis, Improved limits on spin-mass interactions, Phys. Rev. Lett. **120**, 161801 (2018).

[47] T. Jenke *et al.*, A quantized frequency reference in the short-ranged gravity potential and its application for dark matter and dark energy searches, arXiv:1208.3875.

[48] K. Tullney *et al.*, Constraints on spin-dependent short-range interaction between nucleons, Phys. Rev. Lett. **111**, 100801 (2013).

[49] M. Guigue, D. Jullien, A. K. Petukhov, and G. Pignol, Constraining short-range spin-dependent forces with polarized ^{3}He, Phys. Rev. D **92**, 114001 (2015).

[50] Y. K. Feng, D. H. Ning, S. B. Zhang, Z. T. Lu, and D. Sheng, Search for monopole-dipole interactions at the submillimeter range with a ^{129}Xe-^{131}Xe-Rb comagnetometer, Phys. Rev. Lett. **128**, 231803 (2022).

[51] S. Alighanbari, G. S. Giri, F. L. Constantin, V. I. Korobov, and S. Schiller, Precise test of quantum electrodynamics and determination of fundamental constants with HD^+ ions, Nature (London) **581**, 152 (2020).

[52] S. Alighanbari, I. V. Kortunov, G. S. Giri, and S. Schiller, Test of charged baryon interaction with high-resolution vibrational spectroscopy of molecular hydrogen ions, Nat. Phys. **19**, 1263 (2023).

[53] E. Goudzovski *et al.*, New physics searches at kaon and hyperon factories, Rep. Prog. Phys. **86**, 016201 (2023).

[54] V. V. Nesvizhevsky, G. Pignol, and K. V. Protasov, Neutron scattering and extra short range interactions, Phys. Rev. D **77**, 034020 (2008).

[55] Y. Kamiya, K. Itagaki, M. Tani, G. N. Kim, and S. Komamiya, Constraints on new gravitylike forces in the nanometer range, Phys. Rev. Lett. **114**, 161101 (2015).

[56] C. C. Haddock *et al.*, Search for deviations from the inverse square law of gravity at nm range using a pulsed neutron beam, Phys. Rev. D **97**, 062002 (2018).

[57] B. Heacock *et al.*, Pendellösung interferometry probes the neutron charge radius, lattice dynamics, and fifth forces, Science **373**, 1239 (2021).

[58] M. P. Ledbetter, M. V. Romalis, and D. F. Jackson-Kimball, Constraints on short-range spin-dependent interactions from scalar spin-spin coupling in deuterated molecular hydrogen, Phys. Rev. Lett. **110**, 040402 (2013).

[59] V. M. Mostepanenko, A. A. Starobinsky, and E. N. Velichko, The state of the art in constraining axion-to-nucleon coupling and non-Newtonian gravity from laboratory experiments, Universe **6**, 147 (2020).

[60] M. Gorghetto, G. Perez, I. Savoray, and Y. Soreq, Probing *CP* violation in photon self-interactions with cavities, J. High Energy Phys. 10 (2021) 056.

[61] B. A. Dobrescu and I. Mocioiu, Spin-dependent macroscopic forces from new particle exchange, J. High Energy Phys. 11 (2006) 005.

[62] D. F. Jackson Kimball, Nuclear spin content and constraints on exotic spin-dependent couplings, New J. Phys. **17**, 073008 (2015).

[63] P. Fadeev, Y. V. Stadnik, F. Ficek, M. G. Kozlov, V. V. Flambaum, and D. Budker, Revisiting spin-dependent forces mediated by new bosons: Potentials in the coordinate-space representation for macroscopic- and atomic-scale experiments, Phys. Rev. A **99**, 022113 (2019).

[64] V. V. Flambaum and A. F. Tedesco, Dependence of nuclear magnetic moments on quark masses and limits on temporal variation of fundamental constants from atomic clock experiments, Phys. Rev. C **73**, 055501 (2006).

[65] Y. V. Stadnik and V. V. Flambaum, Nuclear spin-dependent interactions: Searches for WIMP, axion and topological defect dark matter, and tests of fundamental symmetries, Eur. Phys. J. C **75**, 110 (2015).

[66] See Supplemental Material at http://link.aps.org/supplemental/10.1103/PhysRevLett.133.113202 for technical details and additional multi-dimensional analysis.

[67] V. A. Dzuba, V. V. Flambaum, I. B. Samsonov, and Y. V. Stadnik, New constraints on axion-mediated P,T-violating interaction from electric dipole moments of diamagnetic atoms, Phys. Rev. D **98**, 035048 (2018).
[68] A. N. Petrov, N. S. Mosyagin, T. A. Isaev, and A. V. Titov, Theoretical study of HfF^+ in search of the electron electric dipole moment, Phys. Rev. A **76**, 030501(R) (2007).
[69] S. V. Khristenko, V. P. Shevelko, and A. I. Maslov, *Molecular Structure* (Springer Berlin Heidelberg, Berlin, Heidelberg, 1998), pp. 1–19.
[70] B. J. Barker, I. O. Antonov, M. C. Heaven, and K. A. Peterson, Spectroscopic investigations of ThF and ThF^+, J. Chem. Phys. **136**, 104305 (2012).
[71] L. V. Skripnikov and A. V. Titov, Theoretical study of ThF^+ in the search for T, P-violation effects: Effective state of a Th atom in ThF^+ and ThO compounds, Phys. Rev. A **91**, 042504 (2015).
[72] K. B. Ng, The ThF^+ eEDM experiment: Concept, design, and characterization, Ph.D. thesis, University of Colorado, Boulder, CO, 2024.
[73] I. Kozyryev and N. R. Hutzler, Precision measurement of time-reversal symmetry violation with laser-cooled polyatomic molecules, Phys. Rev. Lett. **119**, 133002 (2017).
[74] B. L. Augenbraun, Z. D. Lasner, A. Frenett, H. Sawaoka, C. Miller, T. C. Steimle, and J. M. Doyle, Laser-cooled polyatomic molecules for improved electron electric dipole moment searches, New J. Phys. **22**, 022003 (2020).